Synthesis Route to Garnet and Perovskite Thin Films via Quad-Reactive Co-Sputter Deposition of Amorphous Non-Equilibrium Alloy Oxides and Subsequent Annealing

D. Baldwin, 4Wave, Inc., Sterling, VA; M. Martyniuk and R.C. Woodward, The University of Western Australia, Perth, Australia; C.C. Nunes, 4Wave Inc., Sterling, VA; and R.D. Jeffery, Panorama Synergy Ltd., Balcatta, Australia

ABSTRACT

The low temperature reactive sputter deposition of amorphous rare earth substituted Bismuth Iron Garnet $(BiDy)_3(FeAl)_5O_{12}$ using four simultaneous targets via a biased target deposition (BTD) system is reported for the first time. This method provides control over the material composition in a predictable way by controlling the individual target bias. The resultant films deposited on fused quartz substrates are highly uniform and on post annealing form high quality poly-crystalline garnet films.

INTRODUCTION

Rare earth substituted iron garnets have been formed using a variety of techniques including liquid phase epitaxy, chemical phase vapor deposition, magnetron sputtering, pulsed laser deposition, sol gel and reactive ion beam sputtering. The latter have usually been limited to two targets, typically yttrium and iron targets producing yttrium iron garnet (YIG), and have been shown to produce high quality films [1]. It has been shown that substitution of yttrium and iron with bismuth, dysprosium and gallium or aluminum enhance the magneto-optic properties of YIG [2,3]. The control of the composition of films using reactive ion beam sputtering via a single composite metallic target of the four elements is difficult, since the various elements react at different rates in the O_2 atmosphere in the chamber. However, it is shown that using separate targets for bismuth, dysprosium, iron and aluminum in a biased target deposition (BTD) system [4], the composition of the deposited films can be readily controlled. This approach allows the material composition to be easily tailored to suit the application, obviating the need to produce new targets as is required for magnetron sputtering and pulsed laser deposition.

A sketch of the BTD concept is shown in Figure 1. A plasma source in conjunction with a hollow cathode electron source is used to create low energy ions. The ion source is directed at the target to provide ions for sputtering and the target is biased negatively to promote sputtering. A detailed description of the BTD system can be found in [4], however the target arrangement is of particular interest for this application.

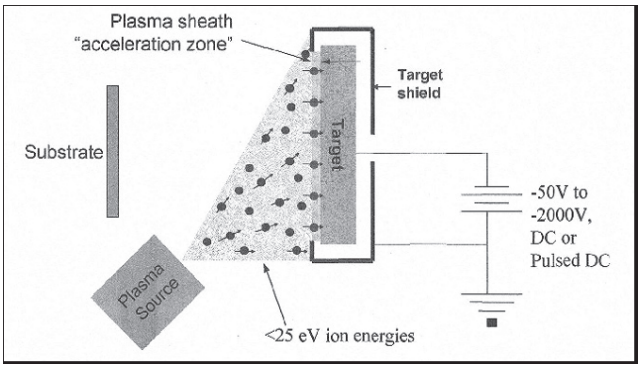

Figure 1: Biased target deposition system concept.

The target assembly caters for six 4" (101.6 mm) diameter targets on a six-sided fixed array as shown in Figure 2. All six targets are positioned for processing, with three targets exposed at any given time and a movable shield provided to prevent cross-contamination. The exposed targets sputter material only if a bias voltage is applied to the target, therefore sputter deposition can occur from one or multiple target materials simultaneously. A configuration like in Figure 2 can be modified to expose a fourth (or fifth and sixth) target at the expense of slight cross-contamination of the targets, which experience has shown is not a problem since sputtering tends to keep each target pure. Each target is water cooled and electrically isolated from the carousel block. The bias may be either DC (metals) or bi-polar pulsed DC (metals and dielectrics). Target voltages are selectable from 10 to 1300V in order to change the energy distribution of the sputtered adatoms. The pulsed DC frequency is variable, up to 71.4 kHz.

An overview of the system control for a single target is shown in Figure 3. The switch drive allows both positive and negative bias voltages, of varying pulse widths, P3 and P4 to be applied to the targets during deposition. The negative voltage attracts positive ions for sputtering while the positive voltage attracts electrons for neutralizing charge build-up on insulating regions.

 505/856-7188
52nd Annual Technical Conference Proceedings, Santa Clara, CA, May 9–14, 2009 ISSN 0737-5921

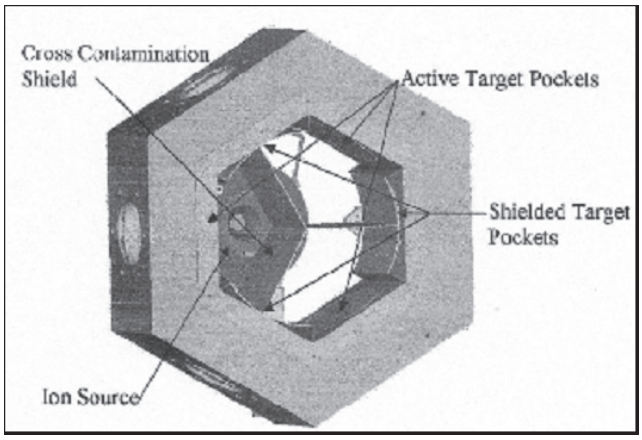

Figure 2: Target configuration in BTD system. The substrate holder (not shown) would be opposite and facing the ion source.

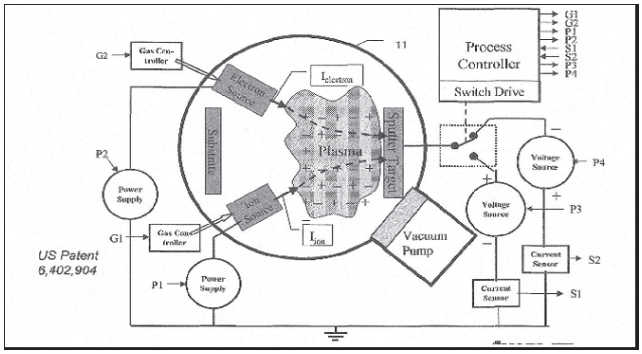

Figure 3: BTD target and plasma control.

EXPERIMENTAL

The experiments were conducted in a commercially available 4Wave, Inc. LANS (Laboratory Alloy Nanolayer Sputtering) system with a stainless steel vacuum vessel pumped by a Helix CT-10 (320 mm dia.) cryo pump. A single Kaufman and Robinson, Inc. (KRI) EH-1000 end-Hall ion source, in conjunction with a KRI model LHC hollow cathode, was used to provide low kinetic energy ion flux to all four sputter targets plus the substrate holder, for substrate sputter pre-cleaning. The plasma source, substrate and all four targets were spaced 4.5 in (114 mm) from the process-center of the chamber, as shown in Figure 2, and the targets were 4 in (101.6 mm) diameter. Gas flows to the sources were regulated and measured by mass flow controllers. Oxygen partial pressure was measured by an Inficon Transpector XPR2 quadrupole mass spectrometer residual gas analyzer (RGA). The RGA was not calibrated for absolute pressure readings, but O_2 partial pressures ranged from 1-5 x 10^{-5} Torr, by proportion of gas flows, in conjunction with overall pressure measurements made by a Granville-Phillips series 354 MicroIon (Bayard-Alpert type) ion gauge. Both RGA and ion gauge were metallically screened from plasma interference. The substrate holder accommodated up to four 1 in (25.4 mm) diameter substrates equally spaced about a bolt circle of 2 in diameter. A retainer clamped the back of the substrates against a silver-filled elastomer conductive pad, which in turn was clamped against a directly water-cooled platen. Estimated maximum temperature rise of the front of the substrates was 80 to 120°C. The platen was spun at 10 rpm during all processing.

Each of the metallic targets produced an oxide when reactively sputtered in the BTD system. Sputtering was done in a mixed Ar/O_2 atmosphere using -850V and +10V, respectively, for the sputtering and neutralizing phases of the bi-polar pulsed DC signal applied to the targets. The frequency of the bi-polar waveform was 71.43 KHz (14 μs per full cycle), the negative or sputtering (mark) portion of the cycle was 11 μs, maximum, while the positive or neutralizing (space) portion of the cycle was 3 μs, minimum. The current drawn, on a long-time average, was ~100 mA and ~200 mA, for the negative and positive portions of the cycle, respectively, at maximum sputtering duty cycle (mark:space) setting. In general, there is an optimum O_2 partial pressure suited to the deposition of each single-metal oxide, such that full oxidation occurs but yet target poisoning does not become excessive and reduction in oxide deposition rate occurs. The optimum O_2 partial pressure for the different metals was measured using the RGA, and the highest of these (PO_2max) was then used in a second round of single-metal oxide depositions to measure the deposition rate for each of the targets at the maximum sputter duty cycle. The Bi target was sputtered at less than maximum duty cycle because its sputter yield was so much higher than that of all the other targets. Note that the higher than optimum O_2 partial pressure resulted in a lower than optimum oxide deposition rate from three of the targets, due to target poisoning, but this cannot be avoided during four-target co-sputtering in a common process environment. Using the maximum duty cycle enabled the deposition flux rate to be readily lowered to adjust the final material composition. For each single-metal oxide film, the effective formula-unit (taken as Fe_2O_3, Bi_2O_3, Dy_2O_3 and Al_2O_3) flux density at the substrate, Φ_{FU} [FU cm^{-2} s^{-1}], obtained at maximum duty cycle, was calculated from the deposition rate expressed as the velocity of the moving growth surface v_{surf} [cm s^{-1}] = final film thickness [cm]/total deposition duration [s] using the relation:

$$\Phi_{FU} = v_{surf} \bullet \rho_{FU}, \quad (1)$$

in which the formula unit density in the solid film, ρ_{FU} [FU cm^{-3}], is given by

$$\rho_{FU} = \rho_{film} \bullet N_A/MW, \quad (2)$$

where ρ_{film} [g cm^{-3}] is the macroscopic density of the film, N_A [FU mole^{-1}] is Avagadro's number and MW [g mole^{-1}] is the gram-molecular weight of the formula unit, i.e., Fe_2O_3, Bi_2O_3, etc. The target duty cycles for each of the targets were then adjusted so that the metal flux density ratios matched the desired stoichiometry, knowing that the final four-metal

alloy oxide would be fully oxidized due to the choice of PO_2max. All four targets were then run simultaneously at their predetermined duty cycles, adjusting the O_2 flow rate to reach PO_2 maximum. After some time (> 10 minutes) of sputtering all four targets at PO_2max, to condition the walls and surroundings inside the process chamber, the substrate shutter was opened and deposition on the substrate(s) was begun. Analysis of the resulting film composition then allows some further minor adjustments to the duty cycles to achieve the exact required stoichiometry.

A simplified example for depositing $Bi_3Fe_5O_{12}$ is shown in Table 1. Here the Fe_2O_3 deposition rate was fixed at 30 A/min. For the same O_2 partial pressure as used for the Fe_2O_3 deposition, the deposition rate of Bi_2O_3 was then measured at a mark-space ratio of the bias voltage (-850V) that put its rate near that of Fe_2O_3. Next the calculation above was performed to account for the differing thin film molar densities of Fe_2O_3 versus Bi_2O_3, expressed as formula unit flux densities. Finally, the desired metals-only composition ratio of the compound $Bi_3Fe_5O_{12}$ was imposed upon the flux densities, keeping the Fe_2O_3 flux constant, and the negative (sputtering) pulse width for the Bi target was adjusted accordingly. Optionally, at this point, a test film can be deposited, analyzed for metals composition and the composition adjusted by changing the formula unit flux densities and recalculating the sputtering pulse widths accordingly. Note that for cases with three or more targets, a unique analytical solution does not exist, but by step-wise fixing and adjusting of parameters, the desired metals percentages can be achieved.

The amorphous $BiDyFeAlO_{12}$ garnet film was sputtered onto a Corning 7980 fused quartz substrate at ~120°C. The chamber pressure was 6.4 x 10^{-4} Torr, the Ar flow rate was 45 sccm and the O_2 flow rate was 4.0 sccm, both introduced through the EH-1000 plasma source. In addition, 10 sccm of Ar was introduced through the LHC hollow cathode but is thought not to be energetically involved in the process. The film deposited over one hour was 3200Å thick giving a sputter rate of 53 Å/min which is similar to the high sputter rates reported for reactive radio-frequency sputtering [1] and comparable with PLD [2,5].

RESULTS

Analysis of the films using Rutherford backscattering spectroscopy (RBS) was performed both before and after annealing (below). Results after annealing are shown in Figure 4. Before annealing, about 2.3 at. % of Ar was trapped in the amorphous structure. After annealing, the Ar content was reduced to 0.66% and the composition was within 1% of the desired composition $(BiDy)_3(FeAl)_5O_{12}$, excluding Ar.

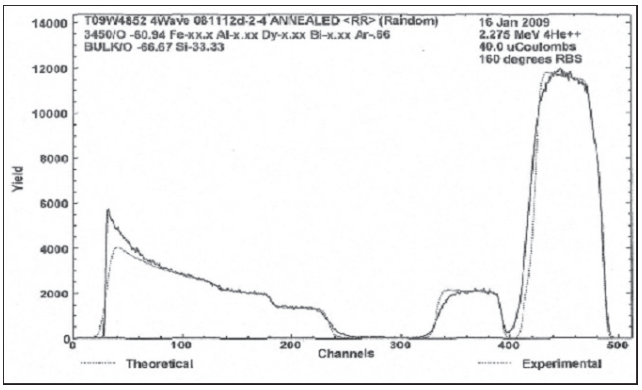

Figure 4: Rutherford backscattering spectrum.

The amorphous film was annealed in a conventional furnace for 1 hour at 650°C in 100% O_2 at atmospheric pressure. RBS on the post annealed film showed that the composition was unchanged within the accuracy of the measurements, and, in particular, the oxygen content of the film was already 60 at. % before annealing in O_2. An X-ray diffraction (XRD) scan of the post annealed film was performed on a Siemens D5000 and the XRD pattern is shown in Figure 5 and shows that a garnet phase has been achieved.

Table 1: Single-metal oxide deposition rates used to calculate target sputtering pulse widths for desired $Bi_3Fe_5O_{12}$ composition, simplified example.

Quantity	**Dimensions**	**Fe_2O_3**	**Bi_2O_3**
Calibration negative pulse width	µs	11	3
Calibration positive pulse width	µs	3	11
Calibration deposition rate	Å/min	30.0	34.8
Reference molar density	moles cm^{-3}	0.032814	0.017945
Reference formula unit density	F.U. cm^{-3}	1.976 x 10^{22}	1.081 x 10^{22}
Calibration formula unit flux density	F.U. cm^{-2} s^{-1}	9.88 x 10^{13}	6.27 x 10^{13}
Goal metals-only atomic percentage	at. %	62.5	37.5
Goal formula unit flux density	F.U. cm^{-2} s^{-1}	9.88 x 10^{13}	5.92 x 10^{13}

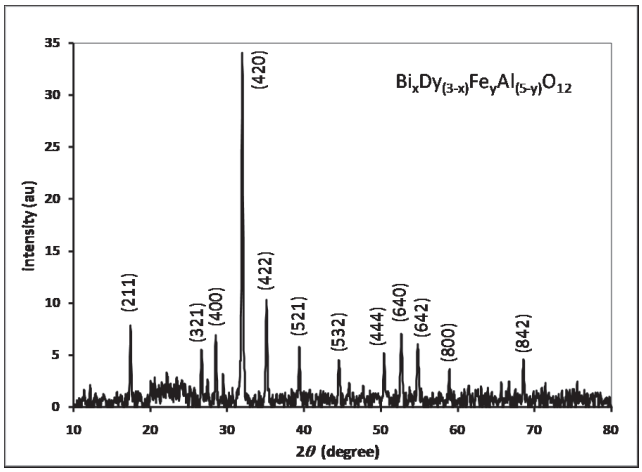

Figure 5: XRD spectrum showing garnet phase on fused quartz substrate.

Hysteresis loops were obtained on films both in plane and perpendicular to the sample surface on a Quantum Design 7 T MPMS SQUID magnetometer at room temperature. The in-plane loop is shown in Figure 6. Once corrected for demagnetizing effects there was no significant difference between the in-plane and perpendicular loops indicating that the samples were magnetically isotropic. The film had a saturation magnetization of approximately 80 kAm^{-1} and a coercivity of about 60 kAm^{-1}, these values are similar to those reported elsewhere [6,7]

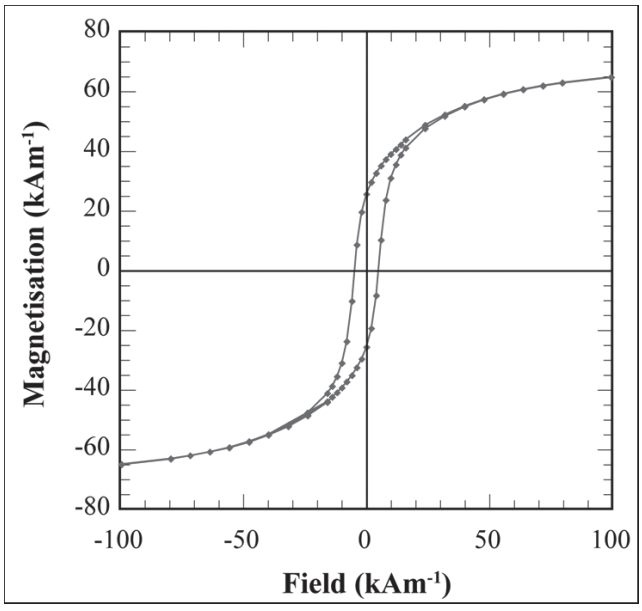

Figure 6: In plane hysteresis loop of $(BiDy)_3(FeAl)_5O_{12}$ from SQUID magnetometer.

Faraday rotation measurements were made using a photo-elastic modulator (PEM) based magneto-optical magnetometer [8]. The Faraday hysteresis loop is similar to the magnetization curve from the SQUID magnetometer and the saturation rotation at 633nm wavelength is 4.4° μm^{-1} again similar to previously published values for similar thin films [6, 7].

CONCLUSIONS

For the first time $(BiDy)_3(FeAl)_5O_{12}$ has been reactively deposited from four metallic targets using biased target deposition. The resulting films are poly-crystalline after annealing and of high quality. This approach allows the film composition to be adjusted by controlling the bias on the individual targets and appears to be suitable for the formation of other complex garnets and perovskites.

REFERENCES

1. S. Sung, X. Qi, B. Stadler, "Integrating yttrium iron garnet onto non garnet substrates with faster deposition rates and high reliability", *Appl. Phys. Lett.* 87, 121111, 2005.

2. S. Kang, S. Yin, V. Adyam, Q. Li, Y. Zhu, "$Bi_3Fe_4Ga_1O_{12}$ Garnet Properties and Its Application to Ultrafast Switching in the Visible Spectrum", *J. Appl. Phys.* 73, 10, 15 May 1993.

3. J. Cho, "Fabrication of Bismuth- and Aluminum-Substituted Dysprosium Iron Garnet Films for Magneto-Optic Recording by Pyrolysis and Their Magnetic and Magneto-Optic Properties", *Korean J. Ceramics*, 1, 2, 91-95, 1995.

4. T. Hylton, B. Ciorneiu, D. Baldwin, et al, "Thin Film Processing by Biased Target Ion Beam Deposition", *IEEE Trans. Magn.* 36, 5, September 2000.

5. R. Lux, A. Heinrich, S. Leitenmeier, et al, "Pulsed-laser deposition and growth studies of Bi3Fe5O12 thin films", *J. Appl. Phys.* 100, 113511, 2006.

6. Y. Zhou, D.F. Shen, F.X. Gan, "Magnetic and magneto-optical properties of Cu doped Bi, Al: DyIG films prepared by the pyrolysis method," *Thin Solid Films*, 227, 193-199, 1993.

7. M Gulliot, H. Le Gall, J.M. Desvignes, M. Artinian, "Analysis of the Dy contribution to the Faraday rotation of Bi-DyIG film", *J. Appl. Phys.*, 81, 5432-5434, 1997.

8. M.N. Deeter, P.A. Williams, "Magneto-optic characterization of Iron garnet crystals using photoelastic modulation", *IEEE Trans. Magn.*, 28, 3234-3236, 1992.